

# Constitutive Model and Elastoplastic Analysis of Structures Under Cyclic Loading

Xucheng Wang, Yutian Lei, Qinghua Du  
*Tsinghua University, Beijing, PRC*

## INTRODUCTION

Many engineering structures in nuclear reactors, thermal power stations, chemical plants and aerospace vehicles are subjected to cyclic mechanical-thermal loading, which is the main cause of structural fatigue failure. Over the past twenty years, designers and researchers have paid great attention to the research on life prediction and elastoplastic analysis of structures under cyclic loading.

One of the key problems in elastoplastic analysis is to construct a reasonable constitutive model for cyclic plasticity. Up to now, a great deal of experimental and theoretical investigation on this subject have been carried out, and lots of models have been proposed (Dafalias, 1976; Eisenberg, 1976; Mróz, 1976; Chaboche, 1977; Drucker, 1981; Valanis, 1983; Ohno, 1986). In practical application, the criterion to evaluate whether a model is reasonable is that the model should have the ability to predict accurately various characteristic behavior of materials, the material constants should be small in number and can be determined conveniently, and the mathematical expression of the model should be sufficiently simple so as to be incorporated easily into computer code and be implemented efficiently. Based on this viewpoint, the authors have proposed a simple model which has the same presentation as the mixed hardening theory (Lei, 1986). The model has only five material constants, excluding those of elasticity, which can be determined by a strain-controlled cycling test. Good agreement has been found between theoretical prediction and experimental data under both strain-controlled and stress-controlled cyclic loading (Lei, 1986; Wang, 1988). Another advantage of this model is that an analytical integration method (Wang, 1985; 1987) may be used instead of numerical approximation to determine stress and plastic strain from deformation results after each iteration or loading increment. It improves the accuracy and efficiency of structural analysis.

In the present paper, the constitutive equations are briefly outlined. Then, the model is implemented in a finite element code to predict the response of cyclic loaded structural components such as a double-edge-notched plate, a grooved bar and a nozzle in spherical shell. Numerical results are compared with those from other theories and experiments.

## CONSTITUTIVE EQUATIONS

Materials demonstrate complicated behavior under cyclic loading, e.g. cyclic hardening, cyclic relaxation, and cyclic creep. In order to simulate these material behavior by constitutive equations, it is necessary to develop a proper hardening law. In other words, the task is to find a reasonable description of both the expansion and the rate of translation of subsequent yield surfaces. Therefore, the equations of the mixed kinematic-isotropic hardening theory may be applied

as the fundamentals of the present theory.

$$F(\sigma_{ij}, \alpha_{ij}, \bar{\epsilon}^P) = \frac{1}{2}(S_{ij} - \alpha_{ij})(S_{ij} - \alpha_{ij}) - \frac{1}{3}k^2(\bar{\epsilon}^P) = 0 \quad (1)$$

$$d\epsilon_{ij}^P = d\lambda \frac{\partial F}{\partial \sigma_{ij}} \quad (2)$$

$$d\alpha_{ij} = \zeta d\epsilon_{ij}^P \quad (3)$$

Equation (1) defines the yield surfaces in stress space.  $S_{ij}$  is the stress deviator,  $\alpha_{ij}$  is the back stress tensor,  $\bar{\epsilon}^P$  is the accumulated effective plastic strain,  $\frac{\sqrt{2}}{3}k$  is the radius of the yield surface. The associated flow rule (2) remains valid when nonproportional effect is not too serious, while the Prager's kinematic hardening law (3) must be redefined to describe cyclic plasticity. From equation (1) to (3) and the consistency condition  $dF=0$ , we have

$$d\lambda = \frac{(S_{kl} - \alpha_{kl}) d\epsilon_{kl}}{2/3k^2(1 + E^P/3G)} \quad (4)$$

$$\zeta = 2/3(E^P - dk/d\bar{\epsilon}^P) \quad (5)$$

where  $G$  is the shear modulus,  $E^P = d\sigma/d\bar{\epsilon}^P$  is the plastic modulus. We may obtain the differential constitutive equations from equations (1) to (5).

$$d\sigma_{ij} = [D_{ijkl}^e - \frac{3G(S_{ij} - \alpha_{ij})(S_{kl} - \alpha_{kl})}{k^2(1 + E^P/3G)}] d\epsilon_{kl} \quad (6)$$

where  $D_{ijkl}^e$  is the elastic stiffness tensor. Equation (6) demonstrates that the two parameters related to the description of cyclic plasticity are  $k$  and  $E^P$ . The determination of these two parameters is based on the understanding of material behavior.

#### Determination of $k$

Experimental data from many alloys show that there is no explicit connection between the size of initial yield surface and that of subsequent yield surfaces. It concludes that the size of the yield surface may have a remarkable change at the first loading reversal. In addition, there is evidence that the size of yield surface at stable limit cycle depends upon the plastic strain amplitude, causing the non-Masing behavior (Jhansale, 1973). Therefore, we have reason to assume that

$$k = k(\bar{\epsilon}^P) = k_s(\Delta \bar{\epsilon}_{max}^P) + [k_0 - k_s(\Delta \bar{\epsilon}_{max}^P)]e^{-h \bar{\epsilon}^P} \quad (7)$$

where  $\frac{\sqrt{2}}{3}k_0$  and  $\frac{\sqrt{2}}{3}k_s$  are initial and stable radius of yield surfaces respectively.  $h$  is a material constant.  $\Delta \bar{\epsilon}^P$  is the plastic strain amplitude. For the sake of simplicity, equation (7) may be specified as a discrete form:

$$k = k_s(\Delta \bar{\epsilon}_{max}^P) + [k_0 - k_s(\Delta \bar{\epsilon}_{max}^P)]e^{-cn} \quad (8)$$

where  $c$  is a material constant.  $n$  denote the number of cycle. Equation (8) means that  $k$  will keep constant at each loading phase. Thus, equation (5) is reduced to  $\zeta = 2/3E^P$  because  $dk/d\bar{\epsilon}^P = 0$ . The constitutive equations in form of purely kinematic hardening.  $k_s(\Delta \bar{\epsilon}^P)$  is determined from the increasing level test.  $k_s(\Delta \bar{\epsilon}_{max}^P)$  gives one possibility of describing the historical effect of maximum strain range  $\Delta \bar{\epsilon}_{max}^P$  on the subsequent response of materials. For materials having Masing's behavior,  $k$  may be considered as a constant for the duration of cyclic loading.

#### Determination of plastic tangent modulus

The most essential features of material behavior have been demonstrated in the former papers (Lei, 1986; Wang, 1988).

(1) The characteristic of monotonic stress-strain curve is independent from that of cyclic stress-strain curve.

(2) Strain-controlled cycles always tend to converge to a stable hysteresis loop after cyclicly hardening or softening. The stable loop usually has zero mean stress. Different hysteresis loops with different strain amplitudes may have the same "Master Curve" (Ellin, 1985).

(3) Stress-controlled cycles may be considered as a particular form of strain-

controlled cycles. Strain-controlled cycled are therefore considered as the essential pattern of cyclic loading.

The key features of material behavior mentioned above is an important basis for the determination of  $E^P$ . Under monotonic loading,  $E^P$  may be determined from monotonic stress-strain curve. Under cyclic loading, stress-strain curves at different loading phase may have a common expression:

$$\bar{\sigma} = E_0^P \bar{\epsilon}^P + \gamma g(\bar{\epsilon}^P) \quad (9)$$

$$E^P = \frac{d\bar{\sigma}}{d\bar{\epsilon}^P} = E_0^P + \frac{d g(\bar{\epsilon}^P)}{d \bar{\epsilon}^P} \gamma \quad (10)$$

where  $\bar{\sigma}$  and  $\bar{\epsilon}^P$  are effective stress and effective strain measured from the current yield point. If there is no plastic strain at the last loading reversal, i.e. the current loading is going from an elastic unloading, they should be measured from the last yielding point.  $\gamma$  is a discrete memory parameter. It remains constant at each loading phase. In stable cycle,  $\gamma = 1$ .  $E_0^P$  is the asymptotic slope of cyclic stress-strain curve. The proposed form of  $g(\bar{\epsilon}^P)$  is:

$$g(\bar{\epsilon}^P) = \frac{\bar{\epsilon}^P}{a \bar{\epsilon}^P + b} \quad (11)$$

where  $a$  and  $b$  are material constants determined from a stable hysteresis loop. Expressions other than (9) to (11) may be applicable, for example, the Ramberg-Osgood law.

Figure 1 illustrates how to determine  $\gamma$ .  $L$  and  $N$  represent the current and the last unloading points. The strain range between  $L$  and  $N$  would uniquely determine a stable hysteresis loop  $L'N'$ , which is formulated by equations (8) and (9) ( $\gamma=1$ ). Starting from  $N$ , it is assumed that the subsequent loading would go through  $D$  and pass across  $LL'$  at point  $F$ , so that

$$\overline{LF} / \overline{LL'} = C_v \quad (12)$$

where  $C_v$  is a material constant describing the rate of cyclic stabilization. It is determined by the relation between stress peaks from experimental data of a strain-controlled test. The stress value is determined by (12). The plastic strain and stress ranges between  $D$  and  $F$  and the discrete parameter  $\gamma$  all satisfy the equation (9). Therefore,  $\gamma$  is determined.

$$\gamma = \frac{\sigma_{DF} - E_0^P \epsilon_{DF}^P}{g(\epsilon_{DF}^P)} \quad (13)$$

$\gamma$  does not change until the subsequent unloading at  $G$ . The next  $\gamma$  should be determined in a similar way.

The simple expression of the model not only makes it easy to be implemented in a computer program but also has its numerical advantage. At each loading increment and iteration, analytical integration method may be applied to calculate plastic strain and stress, with the help of equations (2) to (6), from the increment of displacement and strain. When  $k$  obeys (8) or keeps constant during loading cycle, the model remains the presentation of kinematic hardening law, and the results from analytical integration is accurate. On the other hand, if  $k$  obeys (7), the results from the analytical integration either in the extended form of kinematic hardening (Wang, 1985) or in the form of mixed hardening (Wang, 1987) are sufficiently accurate. Obviously, the analytical integration method is more efficient and more accurate than the conventional numerical approximation.

#### NUMERICAL RESULTS OF FINITE ELEMENT ANALYSIS

Three structural components are considered here, a double-edge-notched plate, which is the same as the one used by Watanabe and Atluri (1985), an axisymmetric notched bar, which has been analyzed by Ohno and Šatra (1987), and an axisymmetric pressure vessel component. These components are subjected to repeated or reversed loading. The material constants used for the notched components correspond to 2024 aluminum (Lei, 1986; Wang, 1988), while those used for pressure vessel component correspond to Grade 10, 20 and A3R mild steel (Lei et al, 1988). The numerical

simulation of the material behavior under uniaxial condition has been performed, and the results have been confirmed to be valid (Lei, 1986; Wang, 1988).

Figure 2, Fig. 3 and Fig. 4 show the finite element models of the grooved bar, the notched plate and the nozzle-shell component respectively. Numerical results of the notched components are shown in Fig. 5 to Fig. 8. They demonstrate that the responses of the grooved bar are similar to that of the notched plate (see also Wang, 1988). Under complete reversed or repeated loading, the stress-strain responses at notch roots are similar to those reported by others (Watanabe, 1985; Chaboche, 1986; Ohno, 1987). Under partially reversed loading, the numerical results (see Fig. 7 and Fig. 8) are similar to the experimental prediction presented by Wetzels (1968), who apply the Neuber's law as unloading condition. Figure 9 shows the principal stress-strain hysteresis loops at the point with maximum stress. These results are also similar to those of notched components.

#### CONCLUDING REMARKS

A constitutive model for cyclic plasticity has been outlined. The mathematical expression of the model is almost as simple as that of the mixed kinematic-isotropic hardening theory except that a simple hardening law in discrete form has been introduced to describe the material behavior under cyclic loading. In many situations, the model can be simplified further into a form of kinematic hardening so that it has only five material constants which may be determined from a strain-controlled test, and the analytical integration method can be applied to improve the accuracy and efficiency of numerical analysis.

Numerical results of two notched components and a nozzle in spherical shell have been compared to those from others. Although the results come from different constitutive theories, i. e. the presented discrete theory, the continuous theory (Chaboche, 1986), the two-surface theory (Ohno, 1987) and the endochronic theory (Watanabe, 1985), they seem to have a similar descriptive ability. It concludes that the presented model is more applicable because its mathematical form and the procedure to determine material constants are simpler.

It is meaningful that the numerical results are similar in principle to those from Wetzels experiment (1968). Further theoretical and experimental investigations are necessary for a further verification of the applicability of constitutive theories. A simplified method for structural analysis replacing the step-by-step approach seems possible, and a further development of the present theory for viscoplasticity is being undertaken.

#### REFERENCES

- Chaboche, J. L. (1977). Bulletin de l'Acad Polonaise des Sciences, Serie Sc. et Tech., Vol.25. No.1. pp.33-42.
- Chaboche, J. L. and Cailletaud, G. (1986). Computers & Structures. vol.23, No.1. pp.23-31.
- Dafalias, Y. F. and Popov, E. P. (1976). J.A.M.(ASME). Vol.43. pp.645-651.
- Drucker, D. C. and Palgen, L. (1981). J.A.M.(ASME). Vol.48. pp.479-485.
- Eisenberg, M. A. (1976). J. Eng. Mater. Technol.(ASME). Vol.98. pp.221-228.
- Ellyin, F. (1985). J. Eng. Mater. Technol. (ASME). Vol.107. pp.119-125.
- Jhansale, H. R. and Topper, T. H. (1973). ASTM STP 519. pp.246-270.
- Lei, Y.-T. and Wang, X.-C. (1986). Proc. 3rd Chinese Congr. Fatigue. Vol.3. pp.1-6
- Lei, Y.-T., Wang, X.-C. and Du, Q.-H. (1988). Pressure Vessel Technol. (ICPVT6). Vol.1. pp.477-484.
- Mróz, Z. Shrivastava, H. P. and Dubbey, R. N. (1976). Acta Mechanica. Vol.25. pp.51-61.
- Ohno, N. and Kachi, Y. (1986). J.A.M. (ASME). Vol.53. pp.395-403.
- Ohno, N. and Šatra, M. (1987). J. Eng. Mater. Technol.(ASME). Vol.109. pp.194-202.
- Valanis, K. C. and Fan, J. (1983). J.A.M. (ASME). Vol.50. pp.789-794.
- Wang, X.-C. and Chang, L.-M. (1985). Proc. SMiRT8. Vol.L. L2/3.

Wang, X.-C. and Chang, L.-M. (1987). Res Mechanica. Vol.20. pp.113-125.  
 Wang, X.-C. and Lei, Y.-T. (1988). Int. Semi. Inelastic Behavior of Solid Models and Utilization. Besançon (France).  
 Watanabe, O. and Atluri, S. N. (1985): J.A.M. (ASME). Vol.52. pp.857-864.  
 Wetzal, R. M. (1968). J. Mater., JMLSA. Vol.3, No.3. pp.646-657.

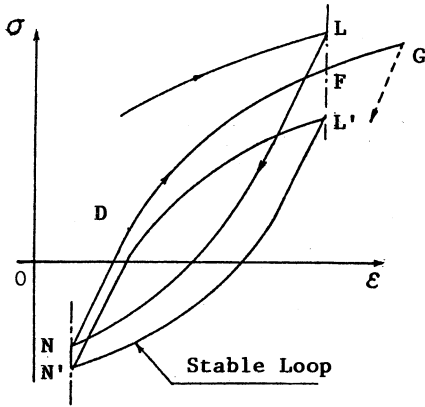


Fig. 1. The determination of  $\gamma$

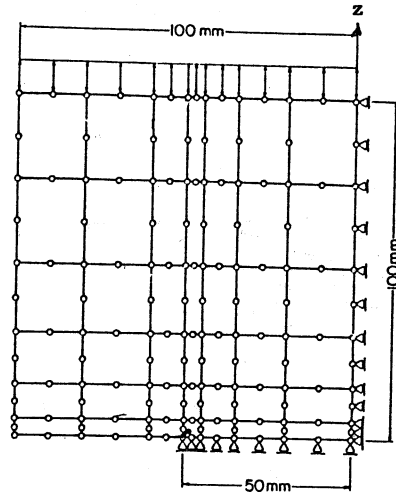


Fig. 3. Finite element model of double-edge-notched plate

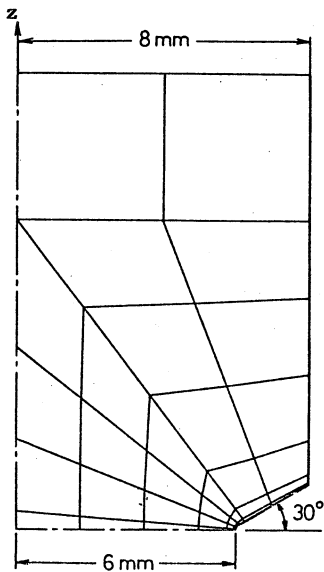


Fig. 2. Finite element model of axisymmetric notched bar

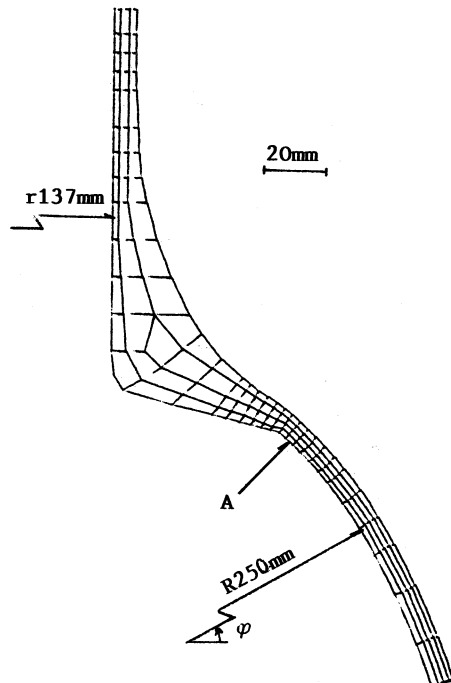


Fig. 4. Finite element model of nozzle in spherical shell

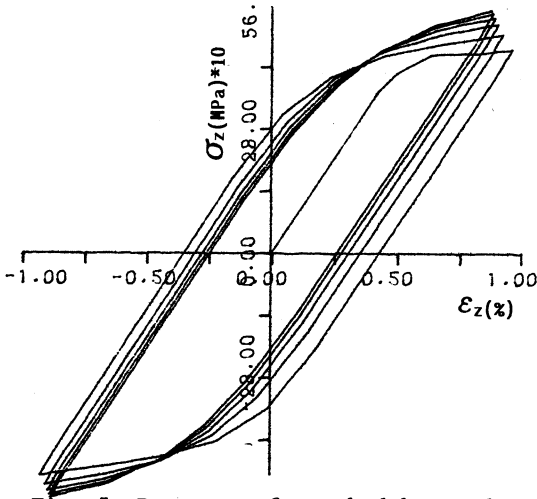


Fig. 5. Response of notched bar under reversed loading (80 MPa --- -80 MPa)

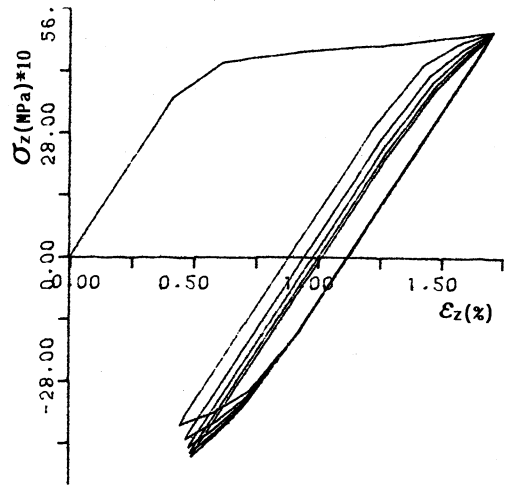


Fig. 6. Response of notched bar under repeated loading (120 MPa --- 0 MPa)

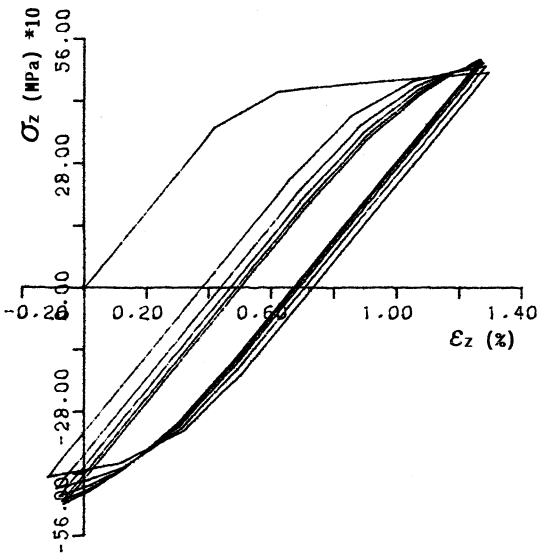


Fig. 7. Response of notched bar under partially reversed loading (100 MPa --- -30 MPa)

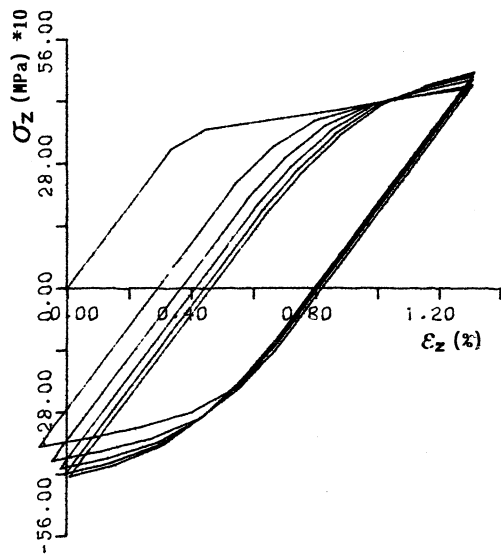


Fig. 8. Response of notched plate under partially reversed loading (140 MPa --- -40 MPa)

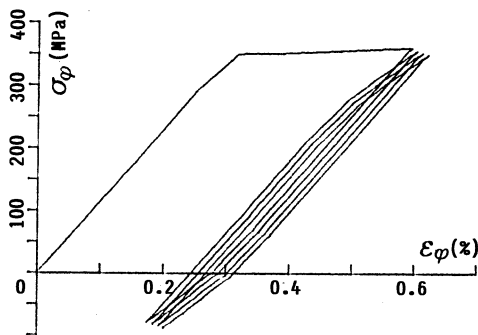


Fig. 9. Response of nozzle-shell connecting under repeated internal pressure (16 MPa --- 0)(point A)